# Chronic Jetlag Accelerates Pancreatic Neoplasia in Conditional *Kras*-Mutant Mice

**Authors:** Patrick B Schwartz, MD[1], Morgan T Walcheck, PhD[1], Manabu Nukaya, PhD[1], Derek M Pavelec, PhD[2], Kristina A Matkowskyj[3,4,5], and Sean M Ronnekleiv-Kelly, MD[1,5]

**Affiliations:**

[1]Department of Surgery, Division of Surgical Oncology, University of Wisconsin School of Medicine and Public Health, Madison, WI

[2]Biotechnology Center, University of Wisconsin, Madison, WI

[3]Department of Pathology and Laboratory Medicine, University of Wisconsin School of Medicine and Public Health, Madison, Wisconsin.

[4]William S Middleton Memorial Veterans Hospital, Madison, Wisconsin.

[5]University of Wisconsin Carbone Cancer Center, University of Wisconsin School of Medicine and Public Health, Madison, WI

**Corresponding Author:** Sean M Ronnekleiv-Kelly, MD (ronnekleiv-kelly@surgery.wisc.edu)

**Address:** 600 Highland Ave. Bx 7375, K3/705 CSC, Madison, WI, 53792

**Phone:** (608) 262-2025 **Fax:** (608) 252-0913

**Running Title:** Chronic Jetlag Accelerates Pancreatic Neoplasia

**Disclosure:** The authors declare no conflict of interest.

**Abstract:**

Pancreatic ductal adenocarcinoma (PDAC) is a devastating cancer with an 80% five-year mortality rate – reflecting an inadequate understanding of pertinent drivers of cancer development. One potential driver of PDAC development is circadian disruption, known to control a myriad of pancreatic processes. Clock dysfunction is associated with multiple risk factors for PDAC, including obesity, diabetes, and heightened inflammation, and has been shown to accelerate the development of other solid-organ cancers. Using a well-characterized model of chronic jetlag (CJ) to mimic irregular sleep patterns, we subjected mice harboring a pancreas-specific activated *Kras* mutation (KC mice) to either a normal lighting pattern or CJ and observed the resultant histopathologic changes. We found that CJ accelerated the development of fibroinflammatory infiltrate/pancreatic intraepithelial neoplasia and increased the grade of the pancreatic lesions. Applying single-cell RNA sequencing over multiple time points, we further identified fibroblasts in the developing pancreatic tumor microenvironment as a putative target of CJ-induced changes. Our results suggest a role for clock dysfunction in PDAC initiation which may hold relevance for preventative efforts.

**Keywords:** Circadian, Pancreas, Jetlag, Pancreatic Ductal Adenocarcinoma, Mouse

## Introduction:

Pancreatic ductal adenocarcinoma (PDAC) is a highly lethal cancer due to its early spread and the limited effectiveness of current therapies. Of the 60,430 people estimated to be diagnosed in 2021, approximately 48,220 (~80%) will die of their disease.[1] This high mortality rate reflects, in part, an inadequate understanding of essential factors driving PDAC development. Insight into these factors could lead to new therapeutic or preventive strategies. One factor that has a strong association with cancer development is the disruption of circadian rhythm caused by irregular sleep patterns.[2]

Circadian clock proteins control daily biological rhythms with an oscillation of 24 hours.[3] Control from the central clock in the hypothalamus assimilates cues from day/night cycles (e.g. sleep patterns) and food intake to modulate peripheral organ rhythmic expression of core circadian genes.[3] In addition to central control, nearly all cells have an autonomous circadian clock based on transcriptional feedback mechanisms of core clock genes (CCGs). Collectively, the CCGs tightly regulate clock-controlled genes (e.g. downstream genes controlled by the clock) that modulate a myriad of cellular processes. Circadian disruption is a condition that affects a substantial proportion of the U.S. population, particularly shift workers and military personnel, whose sleep patterns can be altered dramatically by work schedule requirements.[4] Dysregulation of normal circadian rhythms can result in non-rhythmic and aberrant gene signaling, which can substantially alter organ function and promote various pathologies such as cancer development.[5] Studies have shown a link between circadian disruption and the risk of developing colorectal, lung, and liver cancers, among others.[2,5,6] Furthermore, disruption of this highly regulated process often results in diabetes mellitus, obesity, and increased inflammation- common risk factors for PDAC development.[5,7,8]

We sought to evaluate the effects of a chronic phase shift protocol, known to mimic sleep deprivation (also known as chronic jetlag [CJ]), on PDAC development.[6,9] To accomplish this, we conducted our experiments using the well-established *Kras*$^{G12D/+}$; *Pdx1*-Cre (KC) model of PDAC development.[10] After phase shift protocol, the pancreata of CJ KC mice underwent histopathologic evaluation revealing

increased fibroinflammatory/pre-neoplastic lesions (i.e. pancreatic intraepithelial neoplasia or PanINs) during PDAC development, resulting in increased PanIN grade. Follow-up single-cell RNA sequencing (scRNA-seq) revealed a tumor microenvironment consistent with our histologic analysis. We further identified cancer-associated fibroblasts (CAFs) as the putative target of the effects of CJ. This work serves as a foundation for the understanding of CJ-induced acceleration of PDAC development.

## **Materials and Methodology:**

*Mouse Care and Husbandry*

All animal studies were conducted according to an approved protocol (M005959) by the University of Wisconsin School of Medicine and Public Health (UW SMPH) Institutional Animal Care and Use Committee (IACUC). Male and female mice were housed in an Assessment and Accreditation of Laboratory Animal Care (AALAC) accredited selective pathogen-free facility (UW Medical Sciences Center) on corncob bedding with chow diet (Mouse diet 9F 5020; PMI Nutrition International) and water *ad libitum*.

Conditional *Kras*$^{G12D/+}$ (K) mice (B6.129S4-Kras tm4Tyj/J (#008179)) bred with mice expressing Cre-Recombinase driven by the *Pdx1* promoter (C) (B6.FVB-Tg(Pdx1-cre)6Tuv/J) (#014647)) to generate *Kras*$^{G12D/+}$, *Pdx1*-Cre (KC) mice.[10] The KC mouse has been well characterized previously.[10] To evaluate the effect of loss of clock function on KC mouse pathology the conditional *Arntl*$^{fx/fx}$ mouse, kindly gifted by Professor Christopher Bradfield, was crossed with the KC mouse to generate the *Arntl*$^{fx/fx}$, *Kras*$^{G12D/+}$; *Pdx1*-Cre (AKC) mouse model.[11,12] To identify cell types targeted by *Pdx1*-Cre recombinase in the KC mouse model, the KC mouse was additionally crossed with the conditional Ai14 mouse expressing tdTomato (B6.Cg-Gt(ROSA)26Sortm14(CAG-tdTomato)Hze/J (#007914)) to produce the KCT mouse. The presence of each allele was confirmed with qRT-PCR through Transnetyx (Transnetyx Inc, Cordova, TN). The K, C, and T mice were purchased from Jackson Laboratory (Bar Harbor, ME).

*Chronic Jetlag Protocol*

Starting at 4-6 weeks of age, KC mice were subjected to either a normal circadian (NC) 12-hour light: dark (LD) cycle condition, or a chronic jetlag protocol (CJ) known to mimic altered sleep-wake cycles.[6,9] CJ consisted of a 12-hour LD cycle, phase-shifted forward 4 hours every 2-3 days. Mice were kept under their respective conditions until the study endpoint at 5 and 9 months of age. Kaplan Meier survival analysis between NC and CJ KC mice was made by log-rank testing.

*Histologic Analysis*

Mouse pancreatic tissue was fixed in 10% neutral buffered formalin for 48 hours and then stored in 70% ethanol until slide preparation. Slides were processed, embedded, sectioned, and stained with hematoxylin and eosin (H&E) by the University of Wisconsin Carbone Cancer Center (UWCCC) Experimental Animal Pathology Laboratory (EAPL) Core. All slides were assessed for the presence of precursor lesions (PanIN) along with grading on a scale of 1-3 and/or pancreatic ductal adenocarcinoma (PDAC) by a blinded, board-certified, gastrointestinal pathologist (KAM). Categorical comparisons between groups were made with the Chi-squared or Fisher's Exact test as appropriate. Quantification of the total percent pancreas involvement by the fibroinflammatory infiltrate, atrophy, and/or neoplastic lesions (i.e. PanINs) during the development of PDAC was made by 3 separate reviewers, and differences were tested using Student's t-test between groups. Inter-rater reliability statistics were computed and the intraclass correlation coefficient is reported with associated 95% confidence intervals.

*Immunohistochemistry*

KCT mouse pancreas samples were formalin-fixed, embedded, and sectioned as above by the EAPL Core facility. Immunohistochemistry (IHC) for red fluorescence protein (tdTomato) was also performed by EAPL. Sections were deparaffinized in xylenes and hydrated through graded alcohols to distilled water. Antigens were retrieved using citrate buffer pH 6.0 (10 mM Citric Acid and 0.05% tween 20). Endogenous peroxidase was blocked with 0.3% $H_2O_2$ in PBS for 10 minutes at room temperature and blocking of non-specific binding was performed using 10% goat serum. Sections were incubated with

rabbit anti-RFP antibody (600-401-379, Rockland Inc, Pottstown, PA) (1:1600) overnight at 4ºC. After rinsing, sections were incubated with ImmPRESS goat anti-rabbit IgG (MP-7451, Vector Laboratories, Burlingame, CA) for 30 minutes at room temperature. Detection was performed using the DAB substrate kit (8059S, Cell Signaling Technology, Danvers, MA). Samples were counterstained using Mayer's hematoxylin (MHS32, Millipore-Sigma, St. Louis, MO) for one minute, followed by rinsing and coverslipping of slides.

*scRNAseq Sample Preparation, Library Construction, and Sequencing*

Five- and 9-month-old NC and CJ KC mice were sacrificed with cervical dislocation and the pancreas was rapidly dissected (< 60 seconds) and placed in cold PBS (Thermo Fisher Scientific, Waltham, MA). One male and female pancreas was pooled from each condition and time point. Pancreas samples were minced until the tissue was < 1 mm in diameter, and then centrifuged at 900 RPM for 5 minutes to remove fat contamination. Samples were then incubated with 5 mL of Collagenase P (Sigma Aldrich, St. Louis, MO) in HBSS (Thermo Fisher Scientific) at 37° C for 15 minutes while being shaken at 100 RPM. Additionally, samples were manually agitated every 2-3 minutes. The digestion reaction was quenched with 10 mL R10 media. Samples were then centrifuged at 900 RPM and washed twice with 10 mL of R10. Samples were then strained in a gradient fashion using 500 μm, 100 μm, and 40 μm strainers. Samples were then live/dead sorted into single-cell populations and were transferred to the University of Wisconsin Gene Expression Center (GEC) for Library Preparation.

In brief, libraries were constructed according to the Chromium NextGEM Single Cell 3' Reagent Kit v3.1 User Guide, Rev.D (10x Genomics, Pleasanton, CA). Single-cell suspension cell concentration and viability were quantified on the Countess II (Thermo Fisher Scientific) using 0.4% Trypan Blue (Invitrogen, Carlsbad, CA). Single-cell droplet encapsulation was performed using the Single Cell G Chip and the 10x Genomics Chromium Controller. Following the completion of the Chromium run the GEMs were transferred to emulsion-safe strip tubes for GEM-RT using an Eppendorf MasterCycler Pro thermocycler (Eppendorf, Hamburg, Germany). Following RT, GEMs were broken, and the pooled

single-cell cDNA was collected in Recovery Agent, purified using DynaBeads MyOne Silane beads (Thermo Fisher Scientific), and amplified with the appropriate number of PCR cycles based on the number of cells targeted for recovery. Post-cDNA amplified product was purified using SPRIselect (Beckman Coulter, Brea, CA) and quantified on a Bioanalyzer 2100 (Agilent, Santa Clara, CA) using the High Sensitivity DNA kit. Adapters were then added to the libraries after fragmentation, end repair, A-tailing, and double-sided size selection using SPRIselect. Following adapter ligation, libraries were cleaned up using SPRIselect and sample-specific indexes (Chromium i7 Multiplex Kit, 10x Genomics) were added by sample index PCR using the appropriate number of PCR cycles based on the cDNA yield calculated by the Bioanalyzer quantification. After sample index PCR, samples were double-size selected using SPRIselect and quantified by the Qubit High Sensitivity DNA Kit (Thermo Fisher Scientific). Libraries were sequenced on a NovaSeq6000 (Illumina, San Diego, CA).

*scRNAseq Data Analysis*

Single-cell RNAseq data were analyzed by the UW Bioinformatics Resource Center. Data were demultiplexed using the Cell Ranger Single Cell Software Suite, mkfastq command wrapped around Illumina's bcl2fastq. The MiSeq balancing run was quality-controlled using calculations based on UMI-tools.[13] Sample libraries were balanced for the number of estimated reads per cell and run on an Illumina NovaSeq system. Cell Ranger software was then to perform demultiplexing, alignment, filtering, barcode counting, UMI counting, and gene expression estimation for each sample according to the 10x Genomics documentation (https://support.10xgenomics.com/single-cell-gene-expression/software/pipelines/latest/what-is-cell-ranger). The gene expression estimates from each sample were then aggregated using Cellranger (cellranger aggr) to compare experimental groups with normalized sequencing-depth and expression data.

Gene expression data was then processed using the Seurat version 4 pipeline for data integration.[14] Data was loaded into Seurat. Low quality (<200 features or >20% mitochondrial gene content) and doublets were removed. Cells expressing more than 1% hemoglobin gene content were filtered out. The NC and CJ

KC data were merged and integrated using the SCTransform v2 wrapper with 3000 unique features.[15] SCTransform allows for normalization and better batch correction based on a regularized negative binomial regression. The regression additionally allowed for correction of the cell cycle effect and mitochondrial gene content.[16] A principal component analysis (PCA) was performed with the number of dimensions (principal components) selected based on an elbow plot. Data were visualized using the Uniform Manifold Approximation and Projection for Dimension Reduction (UMAP).[17] Cell identities were called based on the expression of known markers for each cell type and scored using the ScType package to cross-validate identities following the default settings for SCT transformed data in the provided vignette.[18] Differential expression between conditions and time points was performed between clusters or conditions in Seurat using the MAST test based on a log fold change threshold of 0.25 and a false discovery rate (FDR) corrected $p$ value of $p < 0.05$. The MAST test within Seurat is based on the MAST package, which is specifically designed to handle differential expression in scRNA-seq data and utilizes a hurdle model.[19] Gene Set Enrichment Analysis (GSEA) was conducted with the fgsea package leveraged against oncogenic signature gene set (c6.all.v7.5.1.symbols) and biologic process subset of gene ontology (GO BP) (c5.go.v7.5.1.symbols).[20] Pseudotime trajectory analysis was performed with the Monocle 3 package.[21] Genes correlated with pseudotime progression were computed using the Moran's I test and those genes with an FDR $p < 0.05$ were considered significant. \All analyses in this manuscript were conducted in R version 4.2.0 (Vienna, Austria) or GraphPad Prism version 8.3.1 (Dotmatics, Boston, MA).

## **Results:**

*Chronic jetlag promotes pancreatic tumor initiation*

To better understand the effect of chronic jetlag (CJ) on pancreatic cancer development, we elected to utilize the well-characterized *Kras*$^{G12D/+}$, *Pdx1*-Cre (KC) mouse model and assessed the burden of neoplastic lesions (i.e. PanIN and PDAC). All slides were scored for their degree of involvement by 3 independent reviewers with an excellent intraclass correlation coefficient of 0.925 (95% CI 0.911-0.938;

$p < 0.01$). We found that there was a 39.52% increase (12.73% vs. 52.25%) in pancreatic involvement by neoplastic lesions (e.g. PanINs) and the associated fibroinflammatory infiltrate (hereafter referred to as FI/PanIN) from five to nine months in normal circadian (NC) KC mice (**Figure 1A**). Interestingly, KC mice that were exposed to CJ were found to have an approximately 2-fold increase in FI/PanIN at 5 months of development (12.73% vs. 22.47%; **Figure 1A**) – which equilibrated by 9 months (52.25% vs. 43.38%; **Figure 1B**).

After demonstrating CJ increased the degree of FI/PanIN at five months, we evaluated the grade of neoplasia at both five and nine months. Each pancreas was evaluated for PanIN1-3 and PDAC. All NC and CJ KC mice at five and nine months exhibited PanIN1 except a single five-month CJ KC mouse that had evidence of dedifferentiated PDAC which had replaced the entirety of the pancreatic parenchyma (**Figure 2A**). When evaluating higher grade lesions, few mice developed PanIN2-3 or PDAC at 5 months (**Figure 2A**). However, at 9 months, KC mice subjected to CJ had an increased incidence of PanIN2 **(Figure 2B**). Therefore, CJ promoted a greater degree of FI/PanIN initiation leading to increased PanIN grade by nine months.

*Pancreatic clock gene deletion abrogated tumor initiation*

After establishing the effect of CJ on pancreatic tumor development, we next assessed whether circadian disruption within the developing tumor cells similarly demonstrated an accelerated phenotype. We crossed the KC mouse with a conditional deletion of the core clock gene *Arntl* to produce *Arntl*$^{fx/fx}$; *Kras*$^{G12D/+}$; *Pdx1*-Cre (AKC) mice, which possess *Arntl* deletion in cells expressing the *Kras*$^{G12D}$ mutation.[11] *Arntl* is a central transcriptional regulator of the clock and essential for clock functionality.[22] We evaluated the degree of FI/PanIN in NC AKC mice at 5 months and, surprisingly, we found that the lesions had nearly disappeared. Compared to KC mice, AKC mice had an average of 1.59% of pancreatic involvement (vs. 12.73%; $p < 0.01$), and no mice exhibited a higher-grade lesion than a PanIN1 (**Figure 3A**). To understand which cell populations may cause resistance to pancreatic neoplasm formation with loss of *Arntl*, we crossed the KC mouse with the conditional Ai14 mouse expressing tdTomato (**Figure**

**3B**). This revealed tdTomato expression (and thus *Kras*-mutation and *Arntl* deletion) in acinar cells, ductal cells, PanINs and islet cells, with an absence of expression in the fibroinflammatory infiltrate (chronic pancreatitis/atrophy) surrounding the PanINs. Thus, although CJ enhances pancreatic tumor initiation in our mouse model, the loss of *Arntl* expression in pancreatic cells revealed that an intact circadian clock is likely needed to promote the developing pancreatic FI/PanIN.

*Single-cell RNA sequencing of KC mice recapitulates the highly heterogeneous tumor microenvironment*

To better understand how CJ was modulating the pancreatic epithelial cells within the tumor microenvironment to progress toward neoplasia, we evaluated the developing tumor microenvironment over time. To accomplish this, we performed single-cell RNA sequencing (scRNAseq) from pooled pancreatic samples (1 male/female) from both NC and CJ KC mice at 5 and 9 months (**Figure 4B**). After filtering and dimensionality reduction, a total of 14 different heterogeneous cell types were annotated using the ScType package comprising 42,211 cells (**Figure 4A & Supplemental Data 1-2**).[18]

We started by subsetting the pancreatic epithelial cells, which should encompass both normal acinar and developing PanINs, and used pseudotime trajectory analysis to track cell-state changes that occurred from 5 to 9 months. Pseudotime was set to zero at the point with the highest fraction of cells from the 5-month mice and allowed to progress (**Figure 4C**). A Moran's I autocorrelation analysis was then performed to obtain genes that varied across the trajectory (**Supplemental Data 3**). Gene set enrichment analysis (GSEA) of the genes correlated with pseudotime progression was associated with multiple *Kras*-driven cancer cell line signatures – corresponding to the development of pancreatic neoplasia over time (**Figure 4D**). Therefore, we identified a collection of pancreatic epithelial cells that appeared to represent the developing pancreatic cancer microenvironment, which provided a foundation for the subsequent analysis to understand the effects of CJ.

*Chronic jetlag promotes differential clock gene expression in fibroblasts*

We performed DGE across the collective 5- and 9-month mice for differences in core clock gene (CCG) and clock-associated gene expression between the NC and CJ conditions (**Supplemental Data 4**). We hypothesized that clusters with significantly altered expression would be important for downstream investigation. Perhaps most intriguing, the acinar cell/PanIN clusters that we identified and confirmed from the pseudotime analysis did not exhibit DGE. We found that endothelial cells, macrophages, memory CD4 T cells, and monocytes each had a single clock-associated gene differentially expressed (**Figure 5A**). Interestingly, fibroblasts were the only cell type that exhibited DGE of CCGs and clock-associated genes, including *Per2*, *Per3*, *Nr1d2*, *Hlf*, *Tef*, and *Dbp* (**Figure 5A-B**). Fibroblasts are an integral part of the PDAC microenvironment and are known to exhibit circadian rhythmicity when compared to naïve fibroblasts.[23] The lack of other cell types exhibiting changes in clock-specific gene expression suggests fibroblasts may be the target of the CJ-induced accelerated neoplastic phenotype.

*Fibroblasts exhibit time-dependent effects secondary to chronic jetlag*

To further evaluate the fibroblasts within our dataset, we isolated three different subclusters (**Figure 6A**). Using existing markers generated for cancer-associated fibroblasts (CAFs), including inflammatory CAFs (iCAFs), myofibroblast CAFs (mCAFs), and antigen-presenting CAFs (apCAFs), we assigned identities with ScType (**Supplementary Data 5-6**).[24] Of the three clusters, we identified all three as iCAFs – with the expression of known markers, such as *Cle3b*, *Il6*, *Has1*, and *Col14a1* (**Figure 6B**). Notably, fibroblast Cluster 3 exhibited some characteristics consistent with apCAFs, including expression of multiple MHC II components *H2-Aa*, *H2-Eb1*, and *H2-ab1* and *Cd74*, the invariant chain of MHC II (Figure 6B). We then performed DGE and GSEA between NC and CJ iCAFs at 5 and 9 months (**Figure 7A-B** & **Supplemental Data 7**). Consistent with our prior work on the effects of CJ on mouse pancreas, we found that multiple metabolic pathways in fibroblasts were enriched at 5 months (**Figure 7A**).[9,25] Notably, our 9-month comparison revealed enrichment of several apoptosis-related pathways, including 'NEGATIVE_REGULATION_OF_CELL_DEATH' and 'REGULATION_OF_APOPTOTIC_SIGNALING_PATHWAY' (**Figure 7B**). To evaluate if CJ was

simply increasing fibrosis (i.e. collagen deposition) to facilitate these changes, we compared the collagen content from five- and nine-month NC and CJ KC mice (**Supplemental Data 8**). We found no differences in the collagen content at either timepoint. We, therefore, identified that the iCAFs in the developing tumor microenvironment of KC mice had early enrichment of metabolic pathways in response to CJ with late enrichment of apoptosis-related pathways – suggesting CJ augments fibroblast signaling to promote tumor formation.

## **Discussion:**

Pancreatic ductal adenocarcinoma (PDAC) is an aggressive malignancy that has a high rate of mortality.[1] This high rate of mortality is, at least in part, due to an incomplete understanding of the pathogenesis of PDAC. One pathogenic factor being explored in cancers, including PDAC, is the circadian clock.[5,6,26,27] To further evaluate the role of clock dysfunction in PDAC development, we subjected mice to a well-characterized chronic jetlag (CJ) protocol.[9,25] Interestingly, in KC mice prone to PDAC formation, we found that CJ promoted an increase in FI/PanIN development leading to more advanced lesions.[10] We then used a series of scRNAseq experiments to identify fibroblasts as the susceptible cell type to CJ within the developing PDAC tumor microenvironment. Further analysis revealed an enrichment of apoptosis-related pathways, including the negative regulation of cellular death. Future experiments will explore the role of clock dysfunction in promoting alterations in fibroblast signaling and how these alterations promote the acceleration of PanIN formation.

To evaluate the development of PDAC, we selected a well-characterized model of PDAC development, the KC mouse model.[10] Hingorani *et al*. characterized their mice at 2.25, 4.5, and 9 months. They noted that few animals had dysplastic ducts before 5 months of age and higher-grade lesions were rare before 7-10 months. Overall, the group noted few mice developed and succumbed to PDAC (6.89%). Therefore, we selected 5 months as a timepoint where we could potentially note changes in the early initiation of neoplasia during PDAC development, and 9 months to evaluate for the development of higher-grade lesions. Similar to the original description, in mice housed under normal lighting conditions (NC) we

observed that between 5 and 9 months there was an increase in the FI/PanIN lesions. We further identified an increase in the grade of PanIN lesions over time. When we subjected our KC mice to chronic jetlag (CJ), we noted that there was an increase in the amount of FI/PanIN formation (22.47% vs. 12.73%) compared to KC NC mice at 5 months. By 9 months, this appeared to correspond to an increased number of PanIN2 lesions (23.7% vs. 5.1%). Overall, the rate of PDAC was low in either group at nine months (NC = 15.4% vs. CJ = 10.5%). To better understand whether the observed increase in PanIN2 lesions would translate to increased PDAC, a longer follow-up interval or a more aggressive PDAC mouse model outside the current experimental scope (such as the KPC mouse harboring an additional mutation in *Tp53*) would be required.[28] Thus, we identified CJ as a driver of PDAC initiation leading to an increase in PanIN grade. Although previous evidence suggests a role for the clock in PDAC progression, this is the first study to show perturbations in the clock increase tumor initiation in PDAC development.[29,30]

Recently, studies have shown similar effects on initiation in other cancer models. In mice predisposed to colorectal cancer development, mice subjected to constant lighting showed a 2-fold increase in tumor initiation compared to those housed under diurnal conditions.[31] In this study, Stokes *et al*. also showed that global and epithelial loss of *Arntl* recapitulated the increases in tumor initiation, suggesting that *Arntl* is a tumor suppressor in colorectal cancer development and that perturbations in the clock (altered lighting) caused a similar phenotype to clock disruption (*Arntl* deletion). When we crossed our KC mice with the condition *Arntl*$^{fx/fx}$ mouse, we found a discordant phenotype in pancreatic tumor initiation compared to colorectal cancer. Specifically, there was a near abolishment of all FI/PanIN lesions at 5 months (1.59% AKC vs. 12.53% NC KC vs 22.47% CJ KC) – suggesting that an intact *Arntl* is required for the development of PDAC. Previously, in our examination of the effects of CJ on the wildtype pancreatic transcriptome, we found that diurnal rhythmicity was maintained, but widespread changes in metabolic gene expression compared to wildtype NC mice were observed.[9] We also demonstrated that CJ-induced misalignment of LD cues in wildtype mice was associated with changes in the pancreatic lipidome characteristic of pathogenic states, such as diabetes mellitus – a known risk factor for PDAC.[25]

Other investigations have shown that circadian misalignment leads to higher rates of death, changes in cardiac conduction physiology, and hepatocellular carcinoma.[32–35] Thus, although CJ does not cause clock disruption (clock rhythmicity is maintained), misalignment can generate significant pathology. Concordantly, in our model, it is more likely that circadian misalignment – where the internal clock is dyssynchronous with external zeitgebers – rather than arrhythmicity, is the mechanism by which CJ exerts its effects.[32] The findings in our study highlight a key distinction between behavioral models that cause a phase shift in the clock and genetically engineered mouse models causing clock disruption: there may not be an overlap in phenotype owing to differing effects on the clock, or the population of cells impacted by behavioral versus genetic manipulation may be different. For instance, the pancreatic epithelial cells were targeted by the conditional deletion of *Arntl* whereas CJ would ostensibly have a more global impact. Future work will delve into whether conditional clock disruption in the apparent CJ targeted cell population (i.e. fibroblasts) demonstrates a similar or dissimilar phenotype of accelerated pancreatic FI/PanIN development.

To better understand how pancreatic neoplasia progressed in the setting of both NC and CJ conditions, scRNAseq was performed at both 5 and 9 months. We found that the pancreatic epithelial cells, including the PanINs and acinar cells, showed a time-dependent cancer signature on pseudotime analysis consistent with the observed histopathologic changes. Subsequently, when we examined the 14 different cell types for evidence of DGE between NC and CJ, we found that fibroblasts – and not the pancreatic epithelial cells – were the only cell type with multiple CCG and clock-associated gene changes. This finding further supports the notion that CJ augments aspects of the developing tumor microenvironment but not necessarily the epithelial/PanINs themselves. Notably, IHC with KC mice conditionally expressing tdTomato demonstrated that there was *Pdx1*-Cre-directed expression in the acinar, ductal, islet, and PanINs, but not the mesenchymal lineage cells, including the fibroblasts and endothelial cells. Others have also found that clock dysfunction in the supportive stroma of the tumor microenvironment may play a critical role.[36] Alexander *et al*. noted that myeloid-specific deletion of *Arntl* led to increased growth of

melanoma tumors in mice. Furthermore, they found a similar result when they co-injected melanoma along with exogenous macrophages harboring a deletion of *Arntl* compared to wildtype macrophages. Collectively, these data indicated that the supportive components of the tumor microenvironment, such as fibroblasts, may coordinate the observed increases in pancreatic neoplasia secondary to CJ.

When fibroblasts were subsetted in our scRNAseq experiment, we further identified all 3 clusters as inflammatory CAFs (iCAFs) based on known markers.[24] CAFs are known to display differences in rhythmic gene expression compared to naïve fibroblasts.[23] iCAFs secrete IL-6, CXCL9, and TGFβ and can be both immunosuppressive as well as immune promoting.[37] Accordingly, we observed that CJ was associated with enrichment in genes associated with leukocyte motility. Interestingly, we did not observe any differences in the amount of collagen content at 5 or 9 months between NC and CJ KC mice, suggesting a role for paracrine signaling in mediating the effects of CJ by fibroblasts rather than extracellular matrix production (i.e. desmoplasia). After identifying and characterizing the CAFs, we performed GSEA at 5 and 9 months, which demonstrated that at 5 months CJ promoted metabolic gene enrichment – consistent with our prior observations of CJ on wildtype pancreas.[9] However, by 9 months, there was enrichment of multiple cell death and apoptosis-related pathways. Correspondingly, CAFs generate pro-tumor signals to support the developing cancer cells and have been shown to promote decreased cancer cell death and resistance to apoptosis when co-cultured.[38]

Collectively, these experiments shed light on a novel role for the clock in mediating PDAC initiation during development. Future work will be required to elucidate the mechanistic underpinnings which mediate the effects of CJ on PDAC development. Identification of this connection could eventually lead to preventative strategies for patients who are at high-risk for PDAC development, such as those with strong family history or individuals with pancreatic pre-cancerous lesions.

**Figure Legends:**

**Figure 1:** *Pancreatic fibroinflammation/PanIN development is increased by chronic jetlag*. **A.** At 5 months, CJ KC mice (n = 26) and NC KC mice (n= 36) were evaluated for pancreatic fibroinflammation/PanIN (FI/PanIN )development. CJ was found to increase the degree of pancreatic FI/PanIN development compared to NC mice (22.47% vs. 12.73%; $p = 0.027$). **B.** At 9 months the degree of pancreatic FI/PanIN development was not different between CJ mice (n = 39) and NC (n = 33) (43.38% vs. 52.25%; $p = 0.06$).

**Figure 2:** *Chronic jetlag accelerates the grade of PanIN lesions.* KC mice subjected to either NC (black) or CJ (grey) conditions were systematically evaluated for PanINs1-3 and PDAC at 5 (n = 36 vs. n = 26) and 9 months of age (n = 33 vs. n = 39). **A.** At 5 months, few mice exhibited lesions above PanIN1 or PDAC **B.** At 9 months, KC mice subjected to CJ exhibited significantly higher rates of PanIN2 compared to NC KC mice (23.7% vs. 5.1%; $p$ =0.02). **C.** Kaplan Meier log-rank survival was not different between NC (n = 37) and CJ (n = 43) KC mice ($p = 0.31$) during the 9-month study period. **D.** The categorical comparisons between 5- and 9-month KC mice with Fisher's exact testing.

**Figure 3:** *Pancreatic cell deletion of Arntl abrogates pancreatic fibroinflammatory infiltrate/PanIN development*. **A.** Five-month NC KC (n = 36) and NC AKC mice (n = 24) were evaluated for pancreatic fibroinflammation/PanIN (FI/PanIN). Compared to KC mice, AKC mice were found to have their pancreatic FI/PanIN abrogated (12.73% vs. 1.59%; $p = 3.2e-06$). **B.** To evaluate the cell types affected by AKO, KC mice were crossed with Ai14 mice to create KCT mice. H&E stained sections (left) and immunohistochemistry for tdTomato (right) were compared to evaluate cell-specific *Pdx-1* cre expression in KC mice, which was found to be limited to pancreatic epithelial cells, including PanINs (P), acinar (A), islet (I), and ductal (D) cells. Expression was not seen in vascular (V) cells (i.e. endothelial cells) or the fibroinflammatory (F) infiltrate, including fibroblasts and immune cells.

**Figure 4:** *The single-cell landscape of KC mice recapitulates the developing pancreatic cancer tumor microenvironment.* **A.** A total of 14 diverse cell types were identified in the collective single-cell RNA sequencing (scRNAseq) dataset comprising 42,211 cells. **B.** Both 5- and 9-month time points were assayed to correspond to histopathologic analyses. **C.** Pseudotime trajectory analysis was performed for the subset of pancreatic acinar cells with 0 pseudotime set to the point with the highest fraction of cells at 5 months. **D.** Gene Set Enrichment Analysis (GSEA) was performed for the oncogenic signature gene set associated with pseudotime progression and ordered by the log adjusted p value.

**Figure 5:** *Fibroblasts were preferentially affected by chronic jetlag.* **A.** Table of core clock genes (CCGs) and clock-associated genes differentially expressed when comparing NC and CJ conditions of each cell type. **B.** Representative UMAP dimensionality plots demonstrating cellular expression (blue color) of select CCG and clock-associated genes in the subset of fibroblasts.

**Figure 6:** *Fibroblasts subclusters in the developing pancreatic tumor microenvironment were identified as inflammatory cancer-associated fibroblasts.* **A.** A UMAP demonstrating the three fibroblast subclusters identified on dimensionality reduction. **B.** Violin plots with select markers for Pan-, Inflammatory-, Myofibroblastic-, and Antigen Presenting-Cancer Associated Fibroblasts (CAFs). Clusters 1-3 all express markers consistent with Pan-CAFs and Inflammatory CAFs. Cluster 3 also expresses markers consistent with antigen-presenting CAFs.

**Figure 7:** *Chronic jetlag influences fibroblast expression patterns across time.* Figures with The Gene Set Enrichment Analysis (GSEA) demonstrating the gene ontology biologic process (GO BP) pathways enriched in fibroblasts from the NC and CJ conditions at **A.** five and **B.** nine months. The top 10 pathways at each timepoint are ordered by their log-adjusted p value.

**Supplementary Data:**

<u>Supplemental Data 1</u>: Marker database for single-cell RNA sequencing cell-type identification

Supplemental Data 2: ScType Scores for overall single-cell RNA sequencing dataset

Supplemental Data 3: Moran's I pseudotime analysis for the pancreatic acinar cells

Supplemental Data 4: Differential gene expression between normal circadian and chronic jetlag conditions for all cell types

Supplemental Data 5: Marker database for fibroblast subtype identification

Supplemental Data 6: ScType Scores for fibroblast subtype identification

Supplemental Data 7: Differential gene expression between normal circadian and chronic jetlag conditions for fibroblasts at 5 and 9 months

Supplemental Data 8: Quantification of collagen content in 5-month normal circadian and chronic jetlag KC mice

**Acknowledgments:**

We would like to take the opportunity to acknowledge the University of Wisconsin Carbone Cancer Center Support Grant P30 CA014520, which provides funding for the Experimental Animal Pathology Lab Core.

We would also to acknowledge the Gene Expression Center and the Bioinformatics Resource Center (BRC) at the University of Wisconsin, Madison for their contributions to this work.

Finally, we would like to thank the Michael W. Oglesby Foundation for their funding support of our work in circadian disruption and pancreas pathology.

**Grants:**

The research reported in this publication was supported by the Department of Defense Peer Reviewed Cancer Research Program Award CA190176 (Grants.gov ID GRANT12935023) and the University of Wisconsin Institute for Clinical and Translational Research KL2 Award (UL1TR002373 and KL2TR002374) [SRK]. Funding support for this work was also provided by the National Institutes of Health under Award Number T32 ES007015 [PBS]. The content is solely the responsibility of the authors and does not necessarily represent the official views of the National Institutes of Health.

**References:**

1. Siegel RL, Miller KD, Fuchs HE, Jemal A. Cancer Statistics, 2021. *CA Cancer J Clin*. 2021;71(1):7-33. doi:10.3322/caac.21654

2. Schernhammer ES, Laden F, Speizer FE, et al. Night-shift work and risk of colorectal cancer in the nurses' health study. *J Natl Cancer Inst*. 2003;95(11):825-828. doi:10.1093/jnci/95.11.825

3. McIntosh BE, Hogenesch JB, Bradfield CA. Mammalian Per-Arnt-Sim proteins in environmental adaptation. *Annu Rev Physiol*. 2010;72:625-645. doi:10.1146/annurev-physiol-021909-135922

4. Bass J, Lazar MA. Circadian time signatures of fitness and disease. *Science*. 2016;354(6315):994-999. doi:10.1126/science.aah4965

5. Kettner NM, Voicu H, Finegold MJ, et al. Circadian Homeostasis of Liver Metabolism Suppresses Hepatocarcinogenesis. *Cancer Cell*. 2016;30(6):909-924. doi:10.1016/j.ccell.2016.10.007

6. Papagiannakopoulos T, Bauer MR, Davidson SM, et al. Circadian Rhythm Disruption Promotes Lung Tumorigenesis. *Cell Metab*. 2016;24(2):324-331. doi:10.1016/j.cmet.2016.07.001

7. Marcheva B, Ramsey KM, Buhr ED, et al. Disruption of the clock components CLOCK and BMAL1 leads to hypoinsulinaemia and diabetes. *Nature*. 2010;466(7306):627-631. doi:10.1038/nature09253

8. Roenneberg T, Allebrandt KV, Merrow M, Vetter C. Social jetlag and obesity. *Curr Biol*. 2012;22(10):939-943. doi:10.1016/j.cub.2012.03.038

9. Schwartz PB, Walcheck MT, Berres ME, et al. Chronic Jetlag-Induced Alterations in Pancreatic Diurnal Gene Expression. *Physiol Genomics*. Published online May 31, 2021. doi:10.1152/physiolgenomics.00022.2021

10. Hingorani SR, Petricoin EF, Maitra A, et al. Preinvasive and invasive ductal pancreatic cancer and its early detection in the mouse. *Cancer Cell*. 2003;4(6):437-450. doi:10.1016/s1535-6108(03)00309-x

11. Johnson BP, Walisser JA, Liu Y, et al. Hepatocyte circadian clock controls acetaminophen bioactivation through NADPH-cytochrome P450 oxidoreductase. *Proc Natl Acad Sci U S A*. 2014;111(52):18757-18762. doi:10.1073/pnas.1421708111

12. Liu Y, Johnson BP, Shen AL, et al. Loss of BMAL1 in ovarian steroidogenic cells results in implantation failure in female mice. *PNAS*. 2014;111(39):14295-14300. doi:10.1073/pnas.1209249111

13. Smith T, Heger A, Sudbery I. UMI-tools: modeling sequencing errors in Unique Molecular Identifiers to improve quantification accuracy. *Genome Res*. 2017;27(3):491-499. doi:10.1101/gr.209601.116

14. Hao Y, Hao S, Andersen-Nissen E, et al. Integrated analysis of multimodal single-cell data. *Cell*. 2021;184(13):3573-3587.e29. doi:10.1016/j.cell.2021.04.048

15. Choudhary S, Satija R. Comparison and evaluation of statistical error models for scRNA-seq. *Genome Biology*. 2022;23(1):27. doi:10.1186/s13059-021-02584-9

16. Nestorowa S, Hamey FK, Pijuan Sala B, et al. A single-cell resolution map of mouse hematopoietic stem and progenitor cell differentiation. *Blood*. 2016;128(8):e20-e31. doi:10.1182/blood-2016-05-716480

17. McInnes L, Healy J, Melville J. UMAP: Uniform Manifold Approximation and Projection for Dimension Reduction. *arXiv:180203426 [cs, stat]*. Published online September 17, 2020. Accessed February 4, 2021. http://arxiv.org/abs/1802.03426

18. Ianevski A, Giri AK, Aittokallio T. Fully-automated and ultra-fast cell-type identification using specific marker combinations from single-cell transcriptomic data. *Nat Commun*. 2022;13(1):1246. doi:10.1038/s41467-022-28803-w

19. Finak G, McDavid A, Yajima M, et al. MAST: a flexible statistical framework for assessing transcriptional changes and characterizing heterogeneity in single-cell RNA sequencing data. *Genome Biol*. 2015;16. doi:10.1186/s13059-015-0844-5

20. Sergushichev AA. An algorithm for fast preranked gene set enrichment analysis using cumulative statistic calculation. *bioRxiv*. Published online June 20, 2016:060012. doi:10.1101/060012

21. Trapnell C, Cacchiarelli D, Grimsby J, et al. The dynamics and regulators of cell fate decisions are revealed by pseudotemporal ordering of single cells. *Nat Biotechnol*. 2014;32(4):381-386. doi:10.1038/nbt.2859

22. Bunger MK, Wilsbacher LD, Moran SM, et al. Mop3 is an essential component of the master circadian pacemaker in mammals. *Cell*. 2000;103(7):1009-1017. doi:10.1016/s0092-8674(00)00205-1

23. Parascandolo A, Bonavita R, Astaburuaga R, et al. Effect of naive and cancer-educated fibroblasts on colon cancer cell circadian growth rhythm. *Cell Death Dis*. 2020;11(4):289. doi:10.1038/s41419-020-2468-2

24. Elyada E, Bolisetty M, Laise P, et al. Cross-Species Single-Cell Analysis of Pancreatic Ductal Adenocarcinoma Reveals Antigen-Presenting Cancer-Associated Fibroblasts. *Cancer Discov*. 2019;9(8):1102-1123. doi:10.1158/2159-8290.CD-19-0094

25. Schwartz PB, Barrett-Wilt GA, Ronnekleiv-Kelly SM. Chronic Jetlag Alters the Landscape of the Pancreatic Lipidome. *Pancreas*. 2022;51(1):80-89. doi:10.1097/MPA.0000000000001962

26. Relles D, Sendecki J, Chipitsyna G, Hyslop T, Yeo CJ, Arafat HA. Circadian gene expression and clinicopathologic correlates in pancreatic cancer. *J Gastrointest Surg*. 2013;17(3):443-450. doi:10.1007/s11605-012-2112-2

27. Li W, Liu L, Liu D, et al. Decreased circadian component Bmal1 predicts tumor progression and poor prognosis in human pancreatic ductal adenocarcinoma. *Biochem Biophys Res Commun*. 2016;472(1):156-162. doi:10.1016/j.bbrc.2016.02.087

28. Hingorani SR, Wang L, Multani AS, et al. Trp53R172H and KrasG12D cooperate to promote chromosomal instability and widely metastatic pancreatic ductal adenocarcinoma in mice. *Cancer Cell*. 2005;7(5):469-483. doi:10.1016/j.ccr.2005.04.023

29. Jiang W, Zhao S, Shen J, et al. The MiR-135b-BMAL1-YY1 loop disturbs pancreatic clockwork to promote tumourigenesis and chemoresistance. *Cell Death Dis*. 2018;9(2):149. doi:10.1038/s41419-017-0233-y

30. Jiang W, Zhao S, Jiang X, et al. The circadian clock gene Bmal1 acts as a potential anti-oncogene in pancreatic cancer by activating the p53 tumor suppressor pathway. *Cancer Lett*. 2016;371(2):314-325. doi:10.1016/j.canlet.2015.12.002

31. Stokes K, Nunes M, Trombley C, et al. The Circadian Clock Gene, Bmal1, Regulates Intestinal Stem Cell Signaling and Represses Tumor Initiation. *Cell Mol Gastroenterol Hepatol*. 2021;12(5):1847-1872.e0. doi:10.1016/j.jcmgh.2021.08.001

32. West AC, Smith L, Ray DW, Loudon ASI, Brown TM, Bechtold DA. Misalignment with the external light environment drives metabolic and cardiac dysfunction. *Nat Commun*. 2017;8(1):417. doi:10.1038/s41467-017-00462-2

33. Acosta-Rodríguez V, Rijo-Ferreira F, Izumo M, et al. Circadian alignment of early onset caloric restriction promotes longevity in male C57BL/6J mice. *Science*. 2022;376(6598):1192-1202. doi:10.1126/science.abk0297

34. Inokawa H, Umemura Y, Shimba A, et al. Chronic circadian misalignment accelerates immune senescence and abbreviates lifespan in mice. *Sci Rep*. 2020;10. doi:10.1038/s41598-020-59541-y

35. VoPham T, Weaver MD, Vetter C, et al. Circadian Misalignment and Hepatocellular Carcinoma Incidence in the United States. *Cancer Epidemiol Biomarkers Prev*. 2018;27(7):719-727. doi:10.1158/1055-9965.EPI-17-1052

36. Alexander RK, Liou YH, Knudsen NH, et al. Bmal1 integrates mitochondrial metabolism and macrophage activation. *Elife*. 2020;9:e54090. doi:10.7554/eLife.54090

37. Sahai E, Astsaturov I, Cukierman E, et al. A framework for advancing our understanding of cancer-associated fibroblasts. *Nat Rev Cancer*. 2020;20(3):174-186. doi:10.1038/s41568-019-0238-1

38. Olumi AF, Grossfeld GD, Hayward SW, Carroll PR, Tlsty TD, Cunha GR. Carcinoma-associated Fibroblasts Direct Tumor Progression of Initiated Human Prostatic Epithelium1. *Cancer Research*. 1999;59(19):5002-5011.

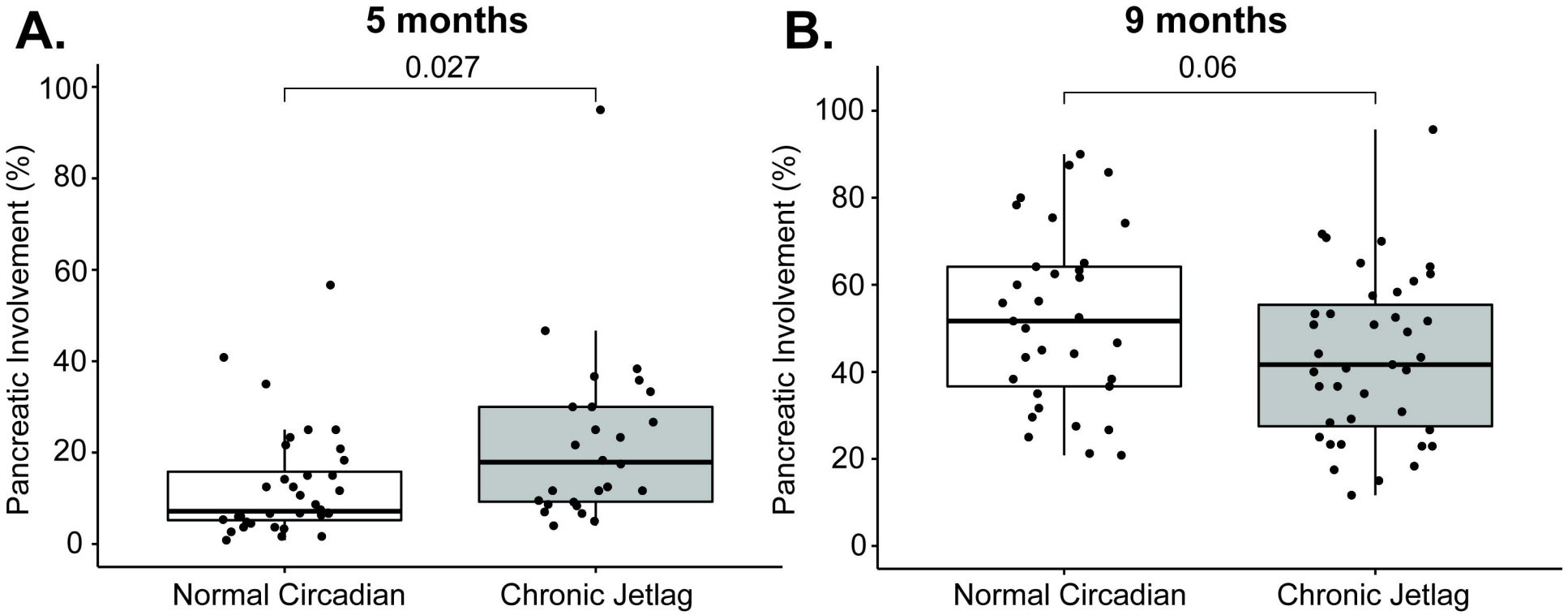
A.
5 months
0.027
Pancreatic Involvement (%)
100
80
60
40
20
0
Normal Circadian
Chronic Jetlag
B.
9 months
0.06
Pancreatic Involvement (%)
100
80
60
40
20
0
Normal Circadian
Chronic Jetlag

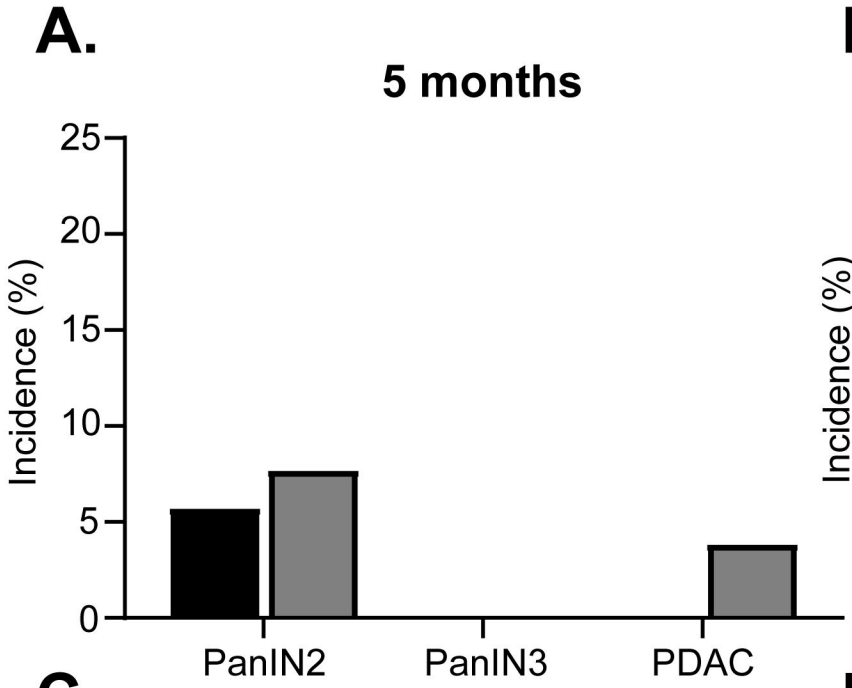


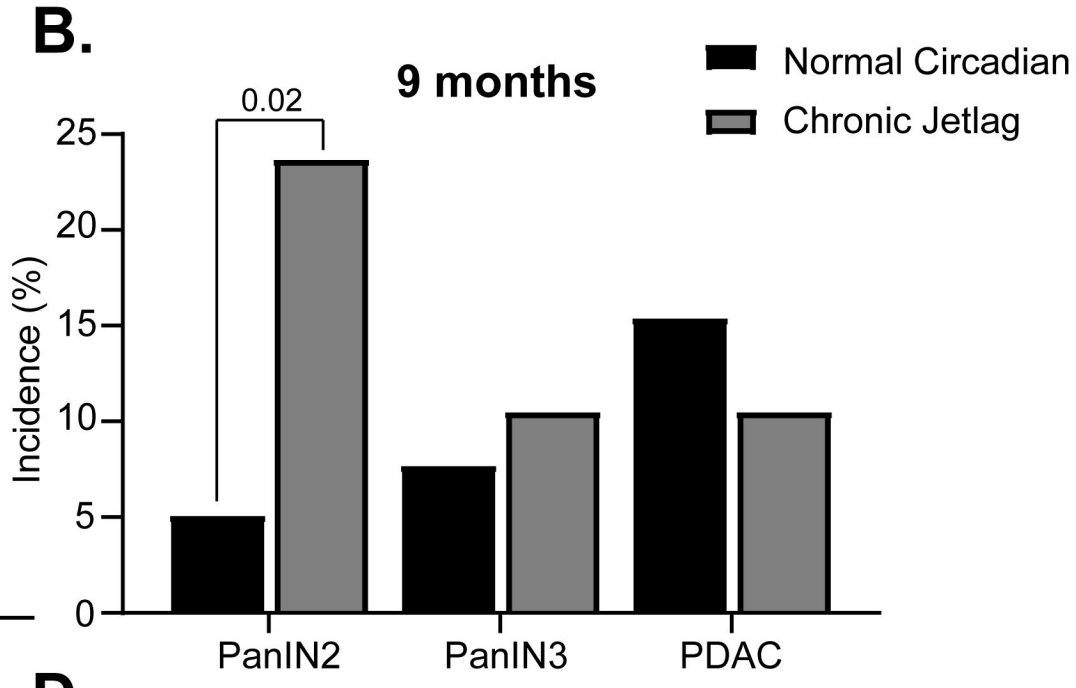


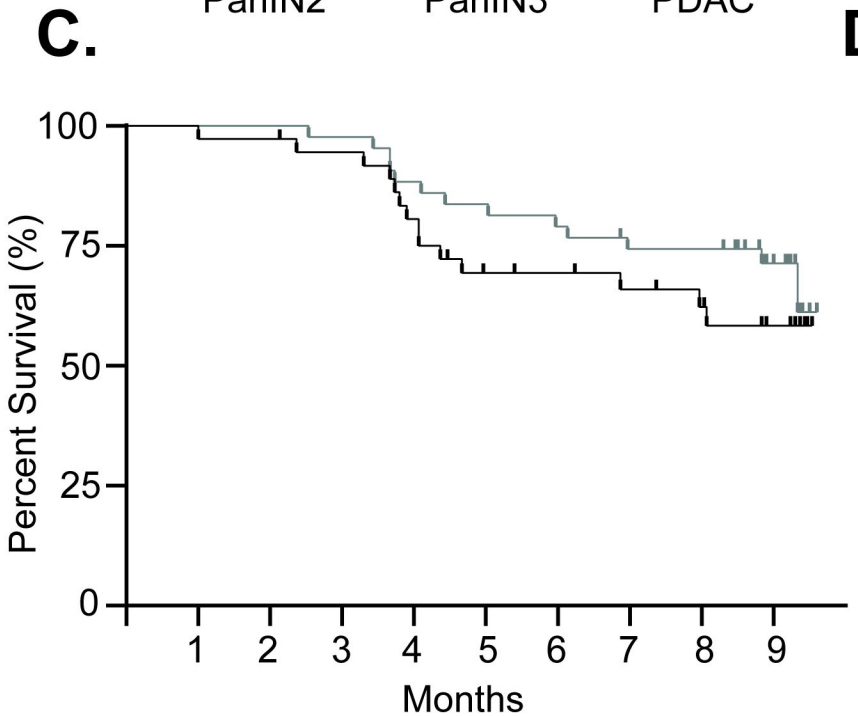


D.

| | 5 months | | | 9 months | | |
|---|---|---|---|---|---|---|
| | **Normal Circadian** | **Chronic Jetlag** | ***p value*** | **Normal Circadian** | **Chronic Jetlag** | ***p value*** |
| PanIN1 | 100% | 96.20% | 0.43 | 100% | 100% | 1.00 |
| PanIN2 | 5.7% | 7.70% | 1.00 | 5.10% | 23.70% | 0.02 |
| PanIN3 | 0% | 0% | 1.00 | 7.70% | 10.50% | 0.72 |
| PDAC | 0% | 3.80% | 0.43 | 15.40% | 10.50% | 0.74 |

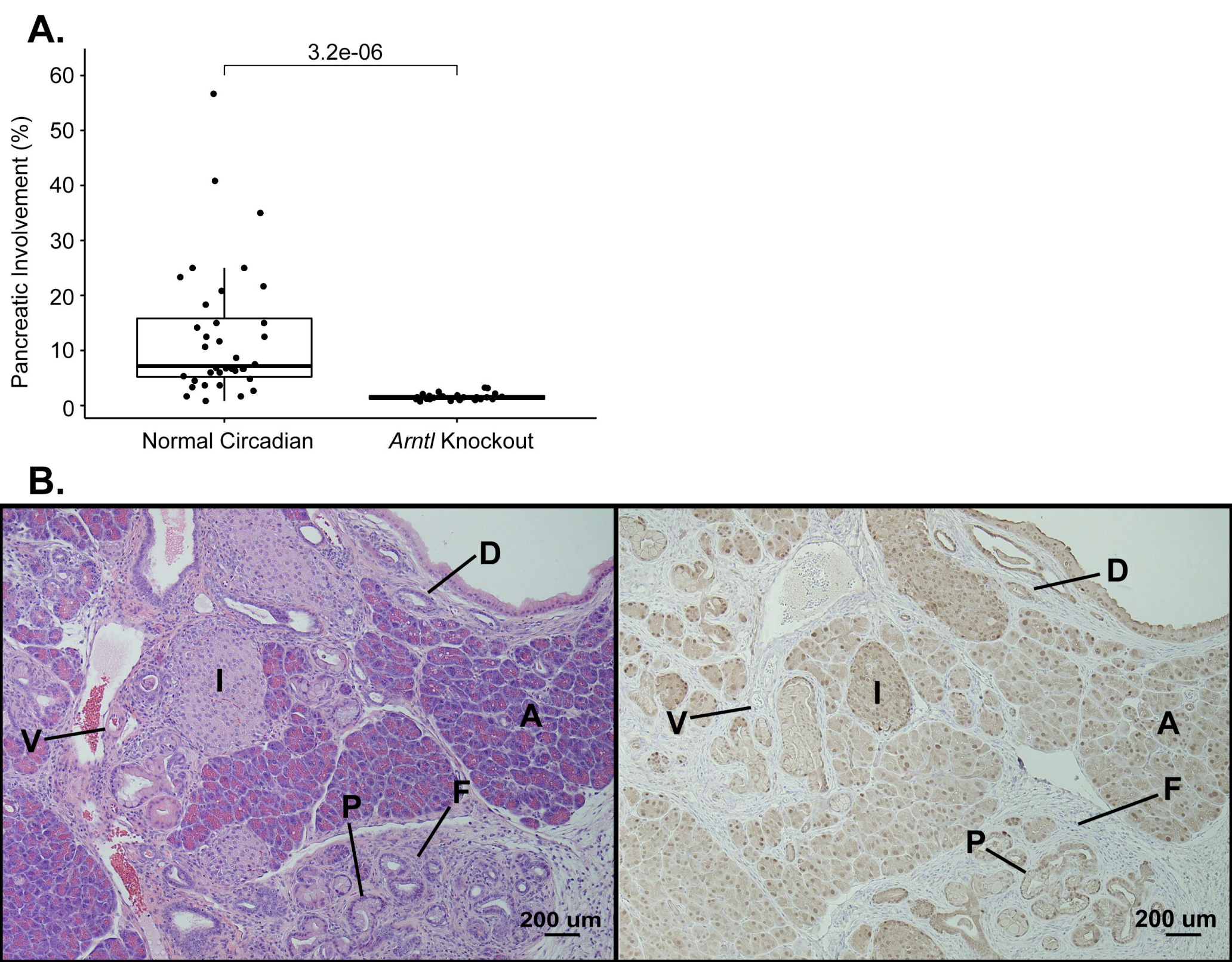
A.
3.2e-06
Pancreatic Involvement (%)
60
50
40
30
20
10
0
Normal Circadian
Arntl Knockout
B.
D
I
V
A
P
F
200 um
D
I
V
A
F
P
200 um

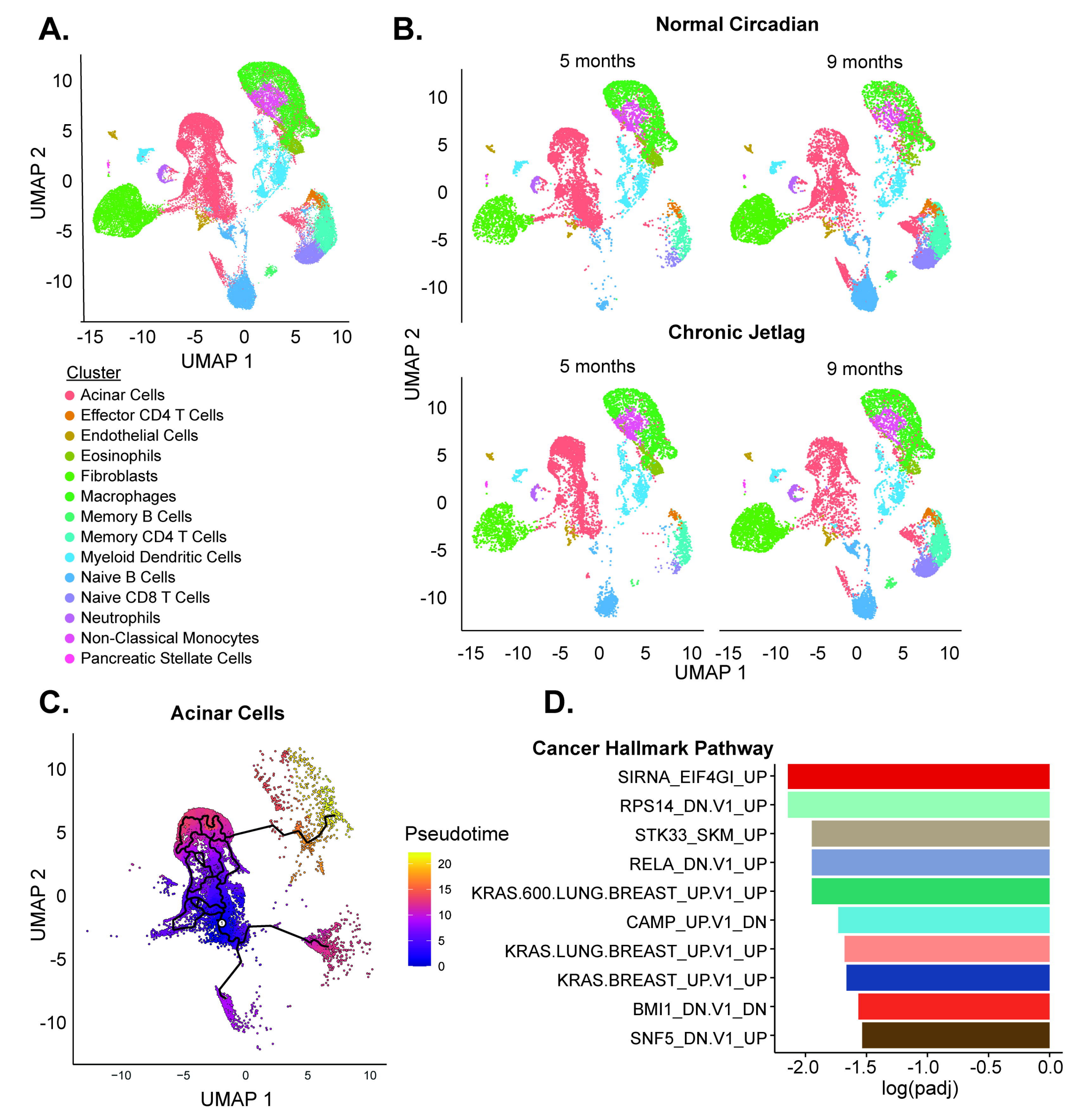
A.
UMAP 2
UMAP 1
Cluster
Acinar Cells
Effector CD4 T Cells
Endothelial Cells
Eosinophils
Fibroblasts
Macrophages
Memory B Cells
Memory CD4 T Cells
Myeloid Dendritic Cells
Naive B Cells
Naive CD8 T Cells
Neutrophils
Non-Classical Monocytes
Pancreatic Stellate Cells
B.
Normal Circadian
5 months
9 months
Chronic Jetlag
5 months
9 months
UMAP 2
UMAP 1
C.
Acinar Cells
Pseudotime
UMAP 2
UMAP 1
D.
Cancer Hallmark Pathway
SIRNA_EIF4GI_UP
RPS14_DN.V1_UP
STK33_SKM_UP
RELA_DN.V1_UP
KRAS.600.LUNG.BREAST_UP.V1_UP
CAMP_UP.V1_DN
KRAS.LUNG.BREAST_UP.V1_UP
KRAS.BREAST_UP.V1_UP
BMI1_DN.V1_DN
SNF5_DN.V1_UP
log(padj)

**A.**

| Cell Type | Gene Name | Log2 FC | Adj p value |
|---|---|---|---|
| Endothelial Cell | *Tef* | 0.326049301 | 0.001081832 |
| Fibroblast | *Dbp* | 0.606422244 | 7.90E-208 |
| Fibroblast | *Per3* | 0.574324977 | 1.74E-209 |
| Fibroblast | *Tef* | 0.395985989 | 2.46E-123 |
| Fibroblast | *Nr1d2* | 0.334812842 | 3.82E-79 |
| Fibroblast | *Hlf* | 0.333177448 | 5.96E-101 |
| Fibroblast | *Per2* | 0.270340607 | 1.22E-130 |
| Macrophage | *Dbp* | 0.425914793 | 4.73E-111 |
| Memory CD4 T Cell | *Bhlhe40* | -0.480979686 | 4.00E-22 |
| Non-Classical Monocyte | *Dbp* | 0.341766669 | 1.68E-18 |

**B.**

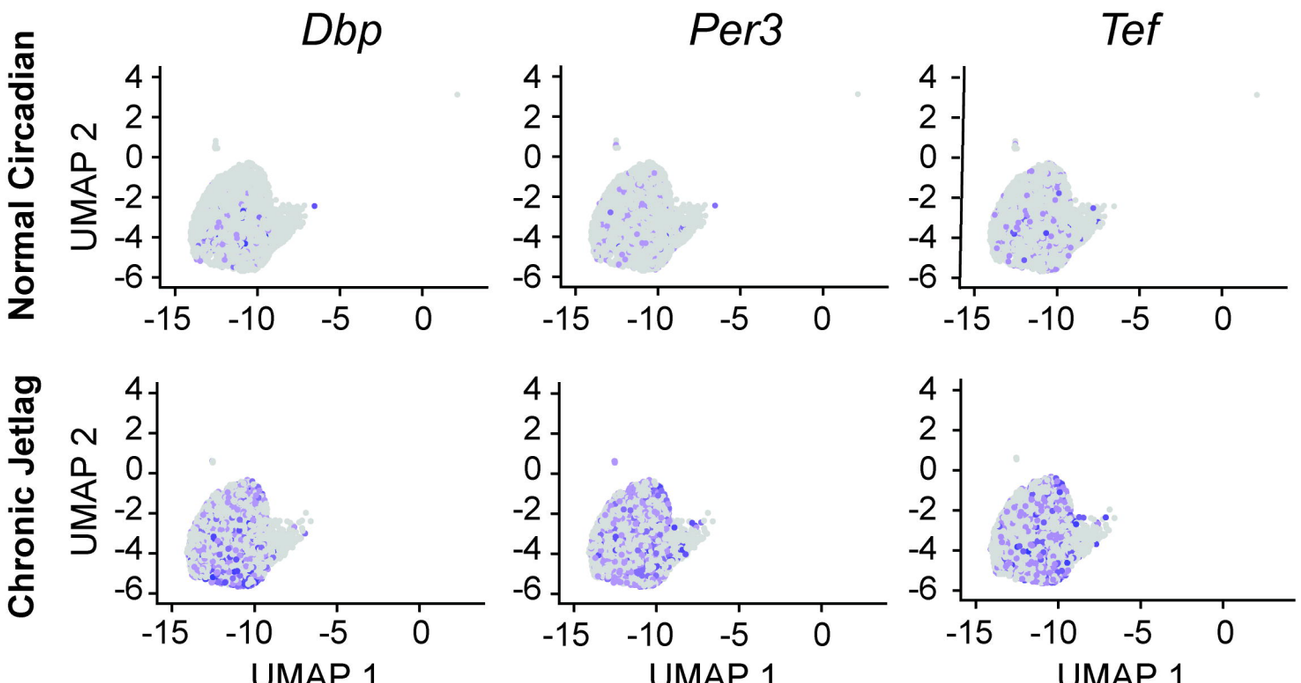

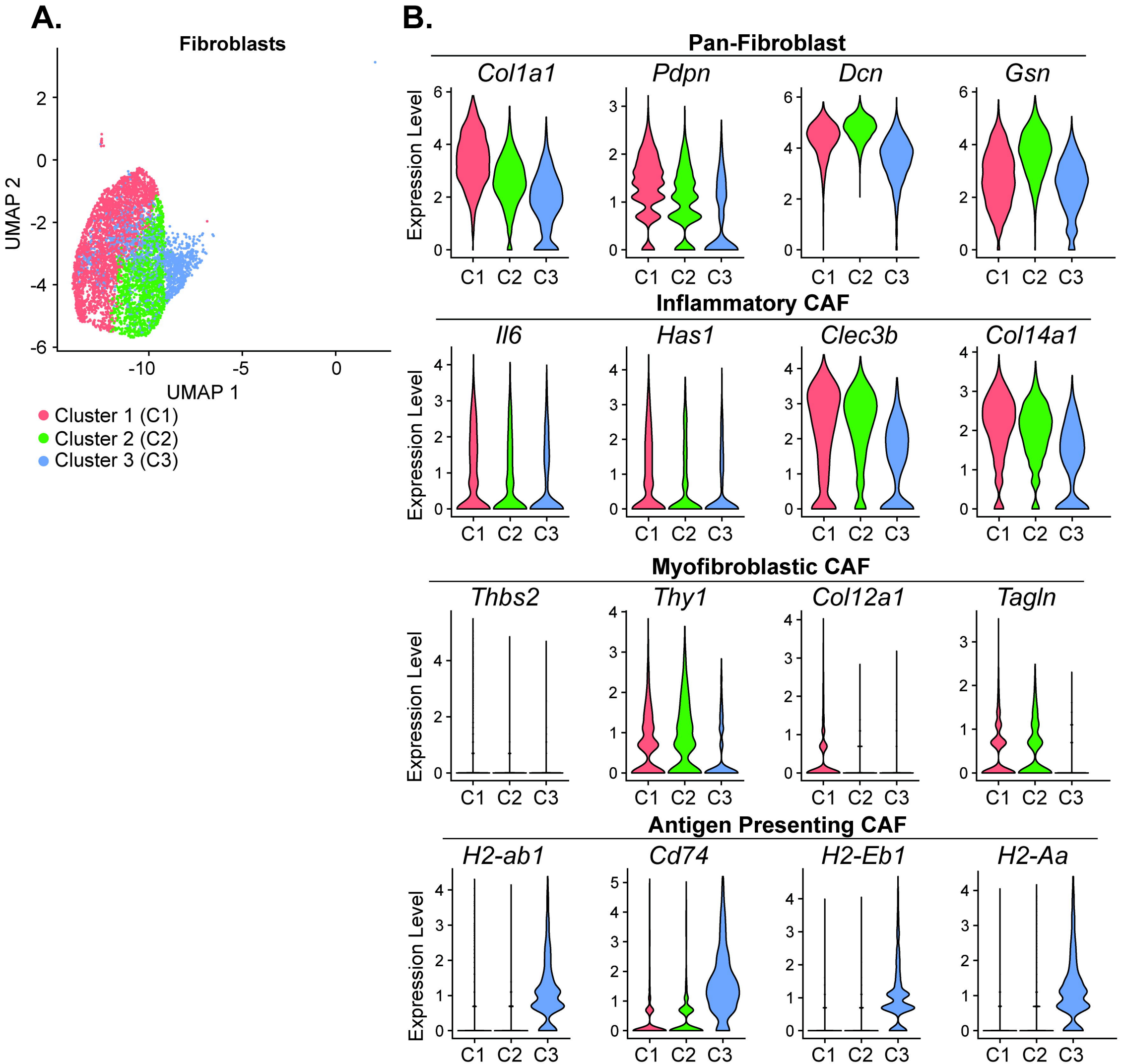
A.
Fibroblasts
UMAP 2
UMAP 1
Cluster 1 (C1)
Cluster 2 (C2)
Cluster 3 (C3)
B.
Pan-Fibroblast
Col1a1
Pdpn
Dcn
Gsn
Inflammatory CAF
Il6
Has1
Clec3b
Col14a1
Myofibroblastic CAF
Thbs2
Thy1
Col12a1
Tagln
Antigen Presenting CAF
H2-ab1
Cd74
H2-Eb1
H2-Aa
Expression Level
C1
C2
C3

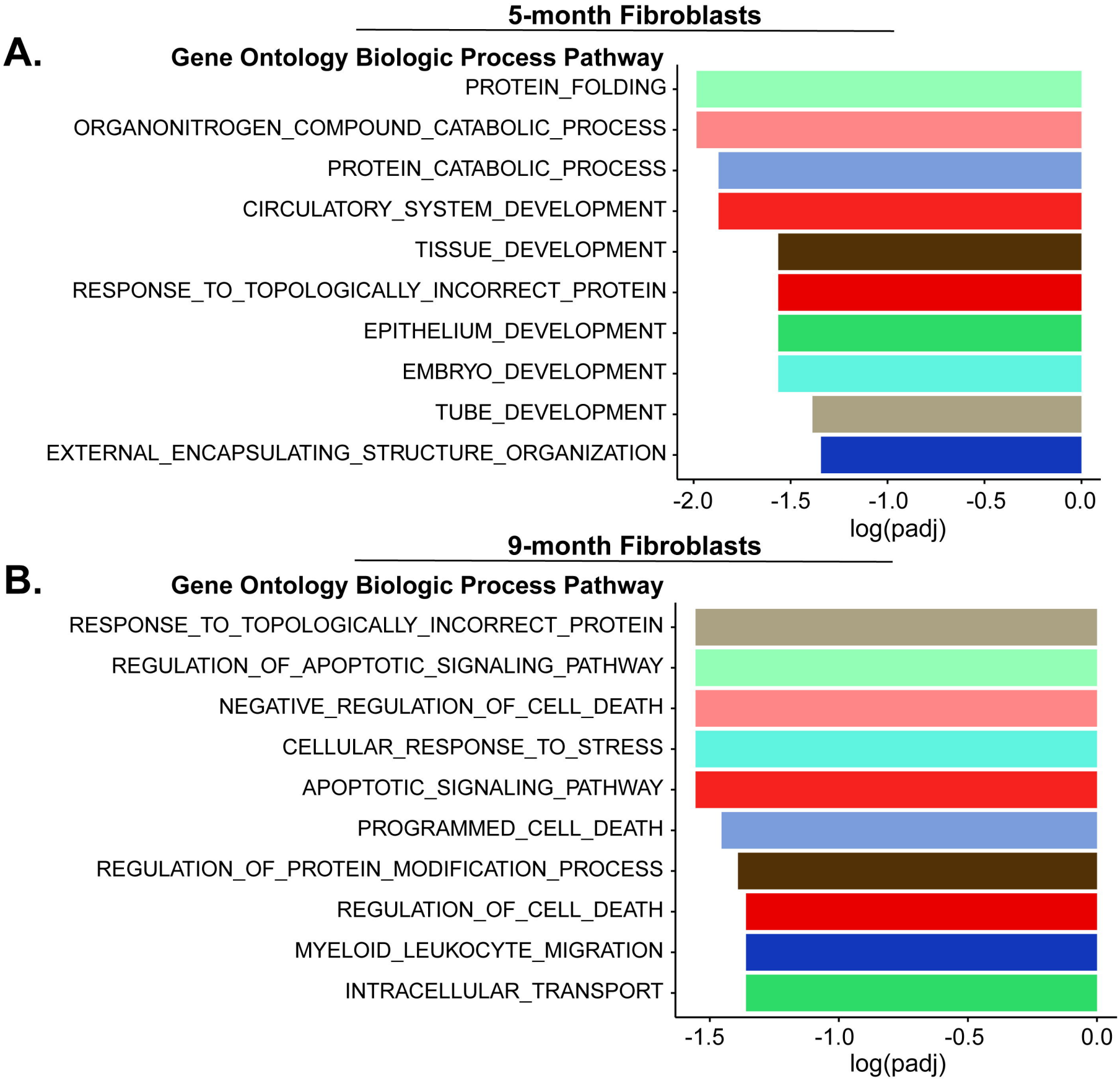
5-month Fibroblasts
A.
Gene Ontology Biologic Process Pathway
PROTEIN_FOLDING
ORGANONITROGEN_COMPOUND_CATABOLIC_PROCESS
PROTEIN_CATABOLIC_PROCESS
CIRCULATORY_SYSTEM_DEVELOPMENT
TISSUE_DEVELOPMENT
RESPONSE_TO_TOPOLOGICALLY_INCORRECT_PROTEIN
EPITHELIUM_DEVELOPMENT
EMBRYO_DEVELOPMENT
TUBE_DEVELOPMENT
EXTERNAL_ENCAPSULATING_STRUCTURE_ORGANIZATION
-2.0
-1.5
-1.0
-0.5
0.0
log(padj)
9-month Fibroblasts
B.
Gene Ontology Biologic Process Pathway
RESPONSE_TO_TOPOLOGICALLY_INCORRECT_PROTEIN
REGULATION_OF_APOPTOTIC_SIGNALING_PATHWAY
NEGATIVE_REGULATION_OF_CELL_DEATH
CELLULAR_RESPONSE_TO_STRESS
APOPTOTIC_SIGNALING_PATHWAY
PROGRAMMED_CELL_DEATH
REGULATION_OF_PROTEIN_MODIFICATION_PROCESS
REGULATION_OF_CELL_DEATH
MYELOID_LEUKOCYTE_MIGRATION
INTRACELLULAR_TRANSPORT
-1.5
-1.0
-0.5
0.0
log(padj)